WAVELET ANALYSIS FOR ESTIMATING THE FRACTAL PROPERTIES OF NEURAL FIRING PATTERNS

C. Heneghan[*,†], S. B. Lowen[†], and M. C. Teich[*,†]

conor@ctr.columbia.edu
steve6@ctr.columbia.edu
teich@enga.bu.edu

[*] *Department of Electrical, Computer and Systems Engineering Boston University, 44 Cummington Street, Boston, MA 02215*
[†] *Department of Electrical Engineering Columbia University, 500 West 120 Street, New York, NY 10027*

ABSTRACT

Fractal stochastic point processes (FSPPs) are useful for modeling the long-term correlations present in the firing patterns of sensory-system nerve fibers. Such processes are characterized by a fractal exponent, which can be estimated in a variety of ways, including a measure based on the statistics of the wavelet transform of the point process. We demonstrate that theoretically, and also in practice, the choice of the wavelet basis is not critical in calculating these statistics, provided some light restrictions on the value of the fractal exponent are satisfied. However, the Haar basis appears to be best as it simplifies calculation, and provides numerical fractal exponent estimates with low standard deviation.

INTRODUCTION

Information in neural systems is carried by trains of action potentials. For an individual nerve fiber, the sequence of action potentials can be well modeled as a stochastic point process. This mathematical construction represents each action potential by its time of occurrence [as shown schematically in Fig. 1(a)]. The point process can alternatively be represented in terms of the derivative of a counting process, $N(t)$, which augments by unity at every instant when an event occurs.

Several statistical measures can be used to identify the form of the point process that describes a neuronal discharge. Two broad classes of statistics are useful: interval-based and count-based measures. Interval-based techniques rely on analysis of the interevent times τ_n illustrated in Fig. 1(a); count-based techniques involve the sequence Z_n generated by counting the number of events in windows of length T [as shown in Fig. 1(b)].

By applying count-based measures to data obtained from primary auditory nerve fibers and visual system neurons in cat (to name but two examples), Teich *et al.* [1,2] showed that the pattern of firing could best be modeled as a *fractal* stochastic point process (FSPP). To the experimental neurophysiologist, fractal nerve spike trains evince a high degree of irregularity in firing (*i.e.*, burstiness even in the face of a steady or absent stimulus), and a slowly converging mean-firing-rate estimate.

Mathematically, such processes possess statistics with power-law behavior. For instance, the count-based power spectral density $S(f)$ of an FSPP varies as $f^{-\alpha}$ over a range of frequency f, where α is defined as the fractal exponent of the process. This exponent provides a useful characterization of the FSPP. We have made extensive use of two count-based measures, the Fano factor $F(T)$ and the Allan factor $A(T)$, as estimators of the fractal exponent. They are defined as [3]:

$$F(T) = \frac{\mathrm{Var}[Z_n]}{\mathrm{E}[Z_n]} \quad \text{and} \quad A(T) = \frac{\mathrm{E}[(Z_{n+1} - Z_n)^2]}{2\mathrm{E}[Z_n]}, \tag{1}$$

where the Z_ns are the sequence of counts and E and Var are the expectation and variance operators, respectively. For an ideal FSPP, the Fano and Allan factors follow the forms

$$F(T) = 1 + (T/T_0)^{\alpha} \quad \text{and} \quad A(T) = 1 + (T/T_1)^{\alpha}, \tag{2}$$

where T_0 and T_1 are defined as fractal onset times.

METHODS

It has recently been shown that the two count-based measures defined above (the Fano and Allan factors) are specific examples drawn from a more general class of multiresolution analysis techniques [3,4], which we have termed the wavelet Fano factor (WFF) and wavelet Allan factor (WAF), respectively. Specifically, the wavelet and scaling transforms of a point process $dN(t)$ are defined, in analogy with those of continuous signals [3,7], as

$$(W_{\psi}N)(a,k) \equiv d[a,k] = a^{-1/2} \int_{-\infty}^{+\infty} \overline{\psi[(u-k)/a]}\, dN(u) \tag{3}$$

and

$$(S_\varphi N)(a,k) \equiv c[a,k] = a^{-1/2} \int_{-\infty}^{+\infty} \overline{\varphi[(u-k)/a]}\, dN(u), \tag{4}$$

where $\psi(t)$ and $\varphi(t)$ are the wavelet and scaling functions respectively, a is a scaling factor, k is a translation factor, $N(t)$ is the counting process, the overbar denotes complex conjugation, and $(W_\psi N)(a,k)$ and $(S_\varphi N)(a,k)$ are the wavelet and scaling transforms of the point process respectively. The WFF and WAF are defined as [3,4]:

$$F_W(a) \equiv a^{1/2} \left(\frac{\mathrm{E}\{\mid c[a,k] \mid^2\} - \mathrm{E}^2\{\mid c[a,k] \mid\}}{\mathrm{E}\{\mid c[a,k] \mid\}} \right), \tag{5}$$

$$A_W(a) \equiv a^{1/2} \left(\frac{\mathrm{E}\{\mid d[a,k] \mid^2\}}{\mathrm{E}\{\mid c[a,k] \mid\}} \right), \tag{6}$$

respectively. The use of the magnitude allows both real and complex valued wavelets to be used.

For the ideal FSPP these two measures vary as [3]:

$$F_W(a) = 1 + (a/A_0)^\alpha \quad \text{and} \tag{7}$$

$$A_W(a) = 1 + (a/A_1)^\alpha \tag{8}$$

where A_0 and A_1 are constants whose values depend on the fractal onset time of the process and the choice of wavelet basis. If the Haar basis [3] is chosen, the WFF and WAF reduce to the ordinary Fano factor and Allan factor, respectively. We proceed to investigate the performance of various wavelet bases in estimating the fractal exponent of an FSPP.

Results

In [3], we showed that the expected value of the WAF for an ideal FSPP is given by

$$A_W(a) = 1 + \frac{\alpha(\alpha+1)}{2} \left(\frac{a}{a_1}\right)^\alpha \int_{-\infty}^{\infty} (W_\psi \psi)(1,z) \mid z \mid^{\alpha-1} dz, \tag{9}$$

where $(W_\psi \psi)(1,z)$ is the continuous wavelet transform of $\psi(t)$ at unit scale, and a_1 is defined in terms of the fractal onset time of the process. Examination of Eq. (9) reveals that $\log A_W(a) = \alpha \log(a) + C_1$, regardless of the choice of wavelet basis, since the integral on the R.H.S. does not depend on a. Accordingly, the fractal exponent can be obtained from a plot of $\log A_W(a)$ vs. $\log(a)$ using any wavelet basis. To ensure the existence of the integral, the condition $\alpha < 2R + 1$ must be satisfied, where R is the number of vanishing moments of the wavelet. Since all admissible wavelet bases have at least one vanishing moment, the WAF will converge for $\alpha < 3$. For the WFF there are no vanishing moments so that the WFF can only be used for $\alpha < 1$. Furthermore, numerical analysis indicates that its estimator has a higher variance [3]. Since the WAF proves useful over a broader range of fractal exponents, we do not consider the WFF further.

The theoretical result embodied in Eq. (9) tells us that all bases are equivalent for calculating the WAF provided that there is an infinite set of $d[a,k]$ on which to calculate the expectations. However, a significant practical issue is how well the variance of a *finite* set of $d[a,k]$ can be estimated for a fractal point process, given the large correlations in $d[a,k]$ for nearby a and k arising from the underlying correlation in the process. Estimating the variance from a set of correlated samples proves difficult [5], since typical variance estimators assume uncorrelated samples. However, a benefit of multiresolution analysis is that the wavelet coefficients are decorrelated relative to the original signal, so that $\mathrm{E}\{d[a,k]\overline{d[a',k']}\}$ decays as $O(\mid ak/a' - k' \mid^{\alpha-1-2R})$, which is analogous to the result as for fBm [6]. Accordingly, the higher R, the less correlation between wavelet coefficients for a given pair $d[a,k]$ and $d[a',k']$, and the more efficient the variance estimator becomes. Unfortunately, increasing the number of vanishing moments is achieved at the expense of effectively widening the support of the wavelet basis, which in turn leads to fewer reliable values of $d[a,k]$ at scale a.

Therefore, in choosing the basis, there is a tradeoff between increasing the value of R to promote decorrelation, and maximizing the number of samples of $d[a,k]$ at a given a. In the numerical simulations reported below, we examine the optimal value of R for certain values of α.

Choice of Basis: Numerical Simulations

The fractal exponents for a set of FSPP simulations were estimated using the WAF calculated with four different wavelet bases: the Haar wavelet, the Daubechies four-tap wavelet, the Daubechies twelve-tap wavelet, and the Morlet wavelet [7]. The first three are real-valued; the last is complex-valued.

In the numerical implementation, the denominator of Eq. (6) is replaced by $\lambda a^{1/2}$, the expected value of $\mid c[a,k] \mid$ [3], where λ is the estimated mean firing rate of the FSPP. The WAFs of a sample data set with a fractal exponent of 0.5, calculated using the four bases described, are shown in Fig. 2; the value of a at which the fractal behavior begins is dictated by the regularity of the wavelet, as well as by the fractal onset time of the underlying process. Figure 3 illustrates the variability associated with estimates of the fractal exponents for a simulated fractal renewal process. This procedure was carried out for three exponents: $\alpha = 0.2$, 0.5, and 0.8. The dot indicates the mean and the bars indicate the standard deviation using the four different wavelet bases. The bias evidenced in estimating the fractal exponent 0.8 is an artifact of the simulation process. Using the student-t test, the values obtained from the four different bases can be shown to be statistically similar; however the variance of the estimates is higher for the higher-R wavelets. Accordingly, the Haar basis appears to offer the best performance in terms of estimating α, as well as providing the most straightforward implementation.

Summary and Conclusions

The wavelet Allan factor can be reliably used to estimate the fractal exponent of an FSPP. The choice of wavelet basis is not critical in the estimation process, provided the fractal exponent is less than $2R+1$, where R indicates the number of vanishing moments for the wavelet. Use of the Haar basis [corresponding to the Allan factor in Eq. (1)] is recommended since its implementation is simpler than for other bases and numerical results indicate that it produces the lowest variance estimate. Use of the Haar basis is also recommended for computing the wavelet Fano factor.

This work was supported by the Office of Naval Research under grant N00014-92-J-1251, by the Joint Services Electronics Program through the Columbia Radiation Laboratory, and by the Whitaker Foundation under Grant No. CU1455801.

References

[1] Teich, M. C. 1989 Fractal character of the auditory neural spike train. IEEE Trans. Biomed. Eng. 36:150–160.

[2] Teich, M. C., Heneghan, C., Lowen, S. B., Ozaki, T., and Kaplan, E. Fractal character of the neural spike train in the visual system of the cat. J. Opt. Soc. Am. A (submitted) preprint.

[3] Teich, M. C., Heneghan, C., Lowen, S. B., and Turcott, R. G. Estimating the fractal exponent of point processes in biological systems using wavelet- and Fourier-transform methods. In *Wavelets in Biology and Medicine*, A. Aldroubi and M. Unser, eds. Boca Raton: CRC Press, 1996.

[4] Abry, P. and Flandrin, P. Point processes, long-range dependence, and wavelets. In *Wavelets in Biology and Medicine*, A. Aldroubi and M. Unser, eds. Boca Raton: CRC Press, 1996.

[5] Beran, J. 1992 Statistical methods for data with long-range dependence. Statistical Science 7:404–427.

[6] 6. Tewfik, A. H. and Kim, M. 1992 Correlation structure of the discrete wavelet coefficients of fractional Brownian motion. IEEE Trans. Inform. Th. 38:904–909.

[7] Vetterli, M. and Kovačević, J. *Wavelets and Subband coding.* Englewood Cliffs, NJ: Prentice-Hall, 1995.

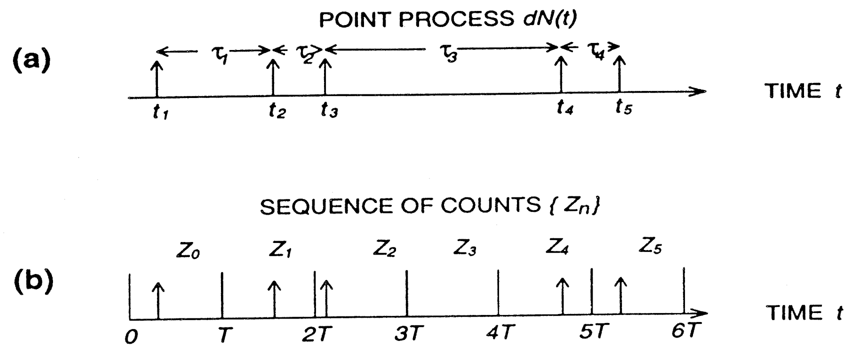

Figure 1: *Representations of a point process. (a) The events are denoted by idealized impulses, occurring at times t_n. (b) The sequence of counts $\{Z_n\}$ is formed from the point process by counting the number of events in successive windows of length T.*

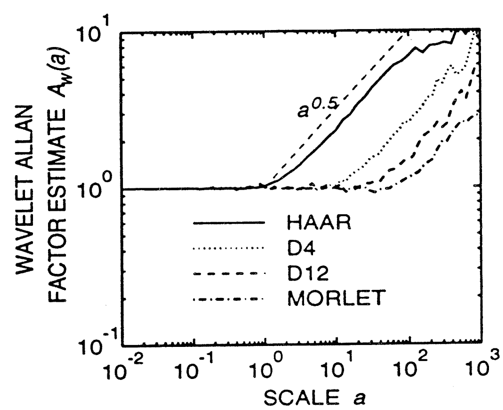

Figure 2: *Wavelet Allan factor estimates using four different wavelet bases, as labeled on graph. The slope of the ideal wavelet Allan factor for this simulated data set is the thin dashed line, which behaves as $a^{0.5}$.*

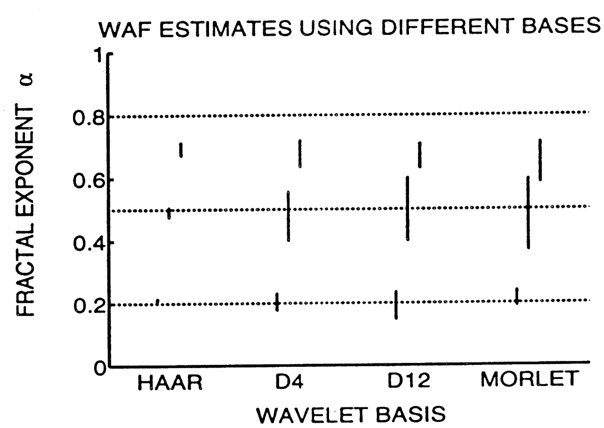

Figure 3: *Mean and standard deviations of a set of WAF estimates for the estimation of α using the four bases shown in Fig. 2. The dotted horizontal lines represent ideal values.*